J. Fluid Mech. (1975), *vol.* 71, *part* 4, *pp.* 701–710
Printed in Great Britain

Measurements in a two-dimensional thermal plume along a vertical adiabatic wall

By J. J. GRELLA AND G. M. FAETH
Mechanical Engineering Department, The Pennsylvania State University, University Park, Pennsylvania 16802

(Received 12 March 1975)

Mean velocities and temperatures were measured in a turbulent plume above a line heat source at the base of a vertical adiabatic wall. Various values of the buoyancy flux and distances above the source in the weakly buoyant regime of the flow were considered. Correlating expressions for the data were determined by assuming streamwise similarity of mean flow quantities, and a fixed entrainment constant and local skin-friction coefficient. The results yielded an entrainment constant based on the average velocity of $0{\cdot}095 \pm 0{\cdot}005$. This value of the entrainment constant is in fair agreement with earlier work on wall plumes, but is less than half the value reported for free line plumes. Local flow properties are only weakly dependent upon the value of the skin-friction coefficient, with variations of 0–0·01 causing only a 3 % change in the mean velocity and weight density defect. The results suggest that the presence of a wall, as opposed to a plane of symmetry, has a strong influence on entrainment, although the specific drag characteristics of the wall are of less importance. The reduced entrainment causes higher velocities and higher values of the weight density defect in a wall plume than in a comparable free plume.

1. Introduction

This investigation considers the wall plume resulting from a line source of buoyancy along the base of a vertical wall. This flow is encountered in the overfire region during the spread of a fire on a vertical surface as well as in other confined natural convection processes. A number of applications of wall plumes on both vertical and sloping surfaces have been discussed by Ellison & Turner (1959) and Turner (1973).

The present study is confined to the turbulent wall plume. Since walls are generally of limited dimensions, only a constant-density ambient environment is considered. Finally, the present investigation treats only the case where the flux of buoyancy within the plume is conserved. For a thermal plume, this implies flow along an adiabatic wall. Conserved buoyancy flux is also a characteristic of unconfined line plumes, and owing to this relationship to the wall plume a comparison will be made between these two flows.

Ellison & Turner (1959) have simulated wall plumes, with conserved buoyancy flux, using saline solutions. The emphasis of their investigation was on the

entrainment characteristics of plumes over walls of various slopes, including vertical walls. For vertical walls, these measurements indicated a substantial reduction in the entrainment of the wall plume from the values reported by Rouse, Yih & Humphreys (1952) and Lee & Emmons (1961) for unconfined line plumes.

Lockwood & Ong (1972) have presented some results on the combustion of a vertical fuel jet along a vertical insulated wall. For a specific combined buoyant and forced flow, the flame length was measured as well as the concentration of an inert contaminant along the wall in the overfire region.

The present work considers, however, a gaseous environment at the limit of the weakly buoyant region, where the influence of the source characteristics is a minimum. Emphasis was placed on the measurement of mean velocity and temperature profiles in order to provide more detail on the structure of the flow than was previously available. Assuming similarity of mean quantities, an analysis is conducted for the weakly buoyant regime. This model provides a basis for correlating the experimental results, determining the entrainment and estimating the influence of wall friction on the flow characteristics.

2. Apparatus

The test apparatus was located in an interior room having plan dimensions of 4×6 m and a ceiling height of 4·5 m. The test wall was 1·22 m wide, 1·91 m high and fitted with side walls 0·61 m wide. The wall was mounted on a base having the same width as the side walls. The front surface of the wall was stainless steel (3·2 mm thick) polished to a nominal r.m.s. surface roughness less than 15 μm. The back of the wall was supported by transite sheet and insulated with fibreglass wool.

The buoyancy source was provided by burning an array of small carbon monoxide jets tangential to the front surface of the wall at its base. The holes for the jets were 2·58 mm in diameter, the spacing between their centres being 6·4 mm.

Gas temperatures were measured using a chromel–alumel thermocouple constructed from 0·025 mm diameter wire. The welded junction had a diameter about 50 % larger than that of the wires and was mounted between heavier support wires 13 mm apart. The fine leads were oriented parallel to the thermal line source in order to minimize conduction errors. A traversing device could position the thermocouple at various distances from the wall with an accuracy of within 0·4 mm.

Mean temperatures were determined by processing the fluctuating thermocouple reading with an integrating digital voltmeter. The probe signal was integrated over a 1 min interval in order to obtain a good average value.

Calibration of the thermocouple system yielded an accuracy of 0·1 °K. This was of the same order of magnitude as the largest radiation correction over the test range so no correction has been employed for radiation.

Velocities were measured with a constant-temperature hot-wire anemometer (Thermo-Systems Model 1050 anemometer and Model 1057 signal conditioner).

Mean values were obtained with the integrating digital voltmeter in the same manner as for the thermocouple signals. A single wire probe with a platinum–rhodium wire 10 μm in diameter and 2·2 mm long was used (DISA Model 55A75). The probe wire was oriented parallel to the thermal source and positioned in the same manner as the thermocouple probe.

The hot-wire system was calibrated using a Thermo-Systems Model 1125 calibrator modified to allow heating of the calibrating air flow over the temperature range of the tests (298–325 °K). For these conditions the concentration of carbon dioxide resulting from combustion was less than 0·2 % and no correction was made for the presence of this contaminant.

Measurements were made along the vertical centre-line of the wall. The flow was substantially two-dimensional. Values of the velocity and temperature defect varied by less than 10 % over distances of up to 0·15 m on either side of the centre-line.

The apparatus was operated for at least 4 h before taking measurements, in order to achieve steady conditions. During the measurement of any profile, the ambient temperature did not vary by more than 0·25 °K.

3. Analysis

The objective of the analysis is to provide a basis for correlating the data and evaluating the effect of wall friction on the flow. The integral equations of conservation of mass, momentum and energy are solved assuming similarity of mean quantities. The entrainment assumption of Morton, Taylor & Turner (1956) is used in the analysis, in analogy with the wall-plume treatment of Ellison & Turner (1959).

The weakly buoyant region of the flow is considered, under the Boussinesq approximation. The flow is two-dimensional, steady and along an adiabatic wall. Denoting distances parallel and normal to the wall by x and y, with corresponding velocities u and v, application of conventional boundary-layer assumptions leads to the following integral forms of the conservation equations:

$$\frac{d}{dx}\int_0^\infty u\,dy = -v_\infty = E, \tag{1}$$

$$\frac{d}{dx}\int_0^\infty \rho u^2\,dy = \int_0^\infty \Delta\gamma\,dy - \tau_0, \tag{2}$$

$$\int_0^\infty u\Delta\gamma\,dy = C_x, \tag{3}$$

where $\Delta\gamma$ is the local weight density defect, E is the net rate of entrainment across the plume boundary, τ_0 is the wall shear stress and C_x is the constant buoyancy flux in the flow. The weight density defect for a local acceleration due to gravity g and local density ρ is given by

$$\Delta\gamma = g(\rho_\infty - \rho), \tag{4}$$

where ρ_∞ is the constant ambient density.

For free turbulent jets and plumes, the assumption of dynamical similarity of mean quantities far from the source is widely accepted. For wall jets and plumes, this assumption is more questionable. Wall-jet measurements by Poreh, Tsuei & Cermak (1967) suggest some Reynolds number dependence, causing departure from similarity near the wall. For turbulent natural convection on an isothermal vertical wall, Cheesewright (1968) also found slightly differing growth rates for the wall layer and the edge of the flow. While it can be detected, the difference in the growth rates is not large, being of order $x^{0.1}$. Furthermore, loss of similarity in the region near the wall does not have a large impact on the integral characteristics of the flow since the zone involved is narrow. Therefore similarity will be assumed in the remainder of the analysis.

Taking $\sigma(x)$ to represent a characteristic width of the flow, the following profile functions are defined:

$$\eta = \frac{y}{\sigma}, \quad \frac{u}{u_m} = f(\eta), \quad \frac{\Delta\gamma}{\Delta\gamma_m} = g(\eta), \tag{5}$$

where $u_m(x)$ and $\Delta\gamma_m(x)$ represent maximum values in the flow at each distance from the source. Also define an entrainment constant similar to that of Morton *et al.* (1956) for free plumes,

$$E = E_0 u_m, \tag{6}$$

and a local skin-friction coefficient,

$$C_f = \tau_0/(\tfrac{1}{2}u_m^2). \tag{7}$$

Both of these factors are based upon the maximum velocity.

With these definitions, the conservation equations become

$$d(u_m \sigma I_1)/dx = E_0 u_m, \tag{8}$$

$$d(2\rho u_m^2 \sigma I_2)/dx = 2\Delta\gamma_m \sigma I_3 - C_f \rho u_m^2, \tag{9}$$

$$u_m \Delta\gamma_m \sigma I_4 = C_x, \tag{10}$$

where

$$\left.\begin{aligned} I_1 &= \int_0^\infty f\,d\eta, \quad I_2 = \int_0^\infty f^2\,d\eta \\ I_3 &= \int_0^\infty g\,d\eta, \quad I_4 = \int_0^\infty fg\,d\eta. \end{aligned}\right\} \tag{11}$$

Ellison & Turner (1959) and, more recently, Turner (1973) assumed that E_0 is a function of the Richardson number only. Under this assumption, E_0 is a constant for a vertical wall. They did note, however, that experimental scatter in E_0 could be attributed to Reynolds number variations, particularly in cases where the layer near the wall was not fully turbulent. In the case of free plumes, Fox (1970) and Narain & Uberoi (1974) have determined an expression for E_0 from the integral form of the moment-of-momentum equation assuming dynamical similarity of mean and turbulent quantities. These results indicate that E_0 is also weakly dependent upon the local Froude number of the flow. Since both the Reynolds number and Froude number effect on E_0 appear to be small, on the basis of the evidence to date, E_0 will be taken to be a constant.

Except for rough walls and high Reynolds numbers, C_f is a function of the Reynolds number. However, the wall friction term is not large in comparison with the buoyancy, and the Blasius correlation for skin friction on a smooth wall suggests a slow variation with Reynolds number. Therefore C_f will also be taken to be a constant in the following.

With these additional assumptions, (8)–(10) can be integrated immediately to yield

$$\frac{\sigma}{x} = \frac{E_0}{I_1}, \quad \frac{u_m}{(C_x/\rho)^{\frac{1}{3}}} = F_m^{\frac{2}{3}}, \quad \frac{\Delta\gamma_m x}{(C_x^2\rho)^{\frac{1}{3}}} = \frac{I_1}{I_4 E_0 F_m^{\frac{2}{3}}}, \tag{12}$$

where F_m is the local Froude number based upon the maximum velocity and is given by

$$F_m = \left[\frac{2I_1 I_3}{2E_0 I_2 I_4 + C_f I_1 I_4}\right]^{\frac{1}{2}}. \tag{13}$$

Under the assumptions of the present analysis, the local Froude number is a constant for a given flow.

For fixed values of E_0 and C_f, equations (12) indicate a linear growth of the plume width, a constant maximum velocity and a maximum weight density defect proportional to x^{-1}. Unconfined line plumes have the same characteristics.

Equations (12) also suggest that a reduction in C_f does not affect the plume width, but results in an increase in the maximum velocity and local Froude number and a reduction in the maximum weight density defect. The higher maximum velocity causes an increase in the net entrainment through (6). These conclusions, however, are based on the assumption that variations in C_f do not influence E_0 and the I_i, which is somewhat speculative at this point.

4. Experimental results

The five sets of test conditions are summarized in table 1. Two heights above the source were considered: 236 and 472 source diameters.

Owing to heat-transfer losses from the flame to the manifold, and radiation from the lower part of the wall, the actual energy flux of the flow was below that computed for complete combustion of the fuel. Therefore the buoyancy flux C_x was determined by direct integration of (3) using the measured velocity and temperature profiles.

The velocity of the fuel gas leaving the manifold was an order of magnitude below the maximum velocities measured at the test locations. This may be seen from table 1 by comparing the local Froude number and the source Froude number, both based upon (13) and the velocities at these points.

If E_0 and C_f are constant and the flow is fully developed, (13) indicates that the local Froude number should be a constant. The values given in table 1 are grouped according to the height over the source and suggest influence of flow development or the Reynolds number on the present results.

The local Reynolds numbers based upon the distance above the source and the measured maximum velocity are also given in table 1. The lower values of the Reynolds number are seen to be associated with lower local Froude numbers. For

Test	x (m)	C_x (N m^{-1} s^{-1})	T_∞ (°K)	ΔT_m (°K)	F_s	F_m	R_{xm}
1	0·61	0·00616	300·3	15·1	0·175	4·45	18 300
2	0·61	0·01330	298·7	24·2	0·258	4·41	23 700
3	1·22	0·00512	300·4	6·0	0·192	5·21	38 300
4	1·22	0·01216	299·9	9·9	0·269	5·52	53 200
5	1·22	0·02998	306·8	18·3	0·471	5·55	70 000

TABLE 1. Summary of the test conditions

the related case of natural convection on a vertical wall, Cheesewright (1968) has found the first appearance of significant turbulent fluctuations to be at a local Reynolds number of 13 500, with fully developed turbulent flow for Reynolds numbers greater than 30 000. The lower Froude numbers in the present measurements also correspond to Reynolds numbers in this range. While complete correspondence between these two flows cannot be anticipated, the possibility that the layer near the wall was not fully developed at the lower wall position cannot be ruled out.

The velocity and weight density defect data for the tests are given in figures 1 (*a*) and (*b*). The co-ordinates for these plots are based on (12). Morton (1959) and Lee & Emmons (1961) have shown that flow-development effects at the source provide a virtual origin for flow similarity that does not correspond to the actual origin of the flow. Owing to the complexity of these factors in the presence of a flame near the source, however, the length scale x used in figures 1 (*a*) and (*b*) has been taken as the uncorrected height along the wall.

Similarity for all positions is only approximate, although the overall variation is no greater than that in the data of Rouse *et al.* (1952) for unconfined line plumes. The present values at the two wall heights are grouped in a systematic fashion as was the case for the local Froude number. In the quasi-steady sense, the trend of this grouping is in agreement with (12). Lower values of the Reynolds number generally imply higher C_f values. Equations (12) indicate that this should result in lower velocities and higher weight density defects with no change in the width scale. These characteristics are generally observed in the figures.

The wall-plume measurements are compared with the data for unconfined line plumes of Rouse *et al.* (1952) in figures 1 (*a*) and (*b*). The latter measurements have been corrected to account for the fact that C_x represents the buoyancy flux in only half of the unconfined flow.

Comparing the two flows shows that a wall plume spreads less rapidly than a free plume. Under a comparable condition, the maximum weight density defect of a wall plume (which is proportional to the maximum temperature rise in the Boussinesq limit) is almost twice that of an unconfined line plume. This implies that wall plumes are more effective in preheating the wall during fires than would have been anticipated on the basis of free-plume measurements. The reduced rate of spread more than compensates for the effect of wall drag on plume velocities. Velocities in a wall plume are higher than those in an unconfined line plume under comparable conditions.

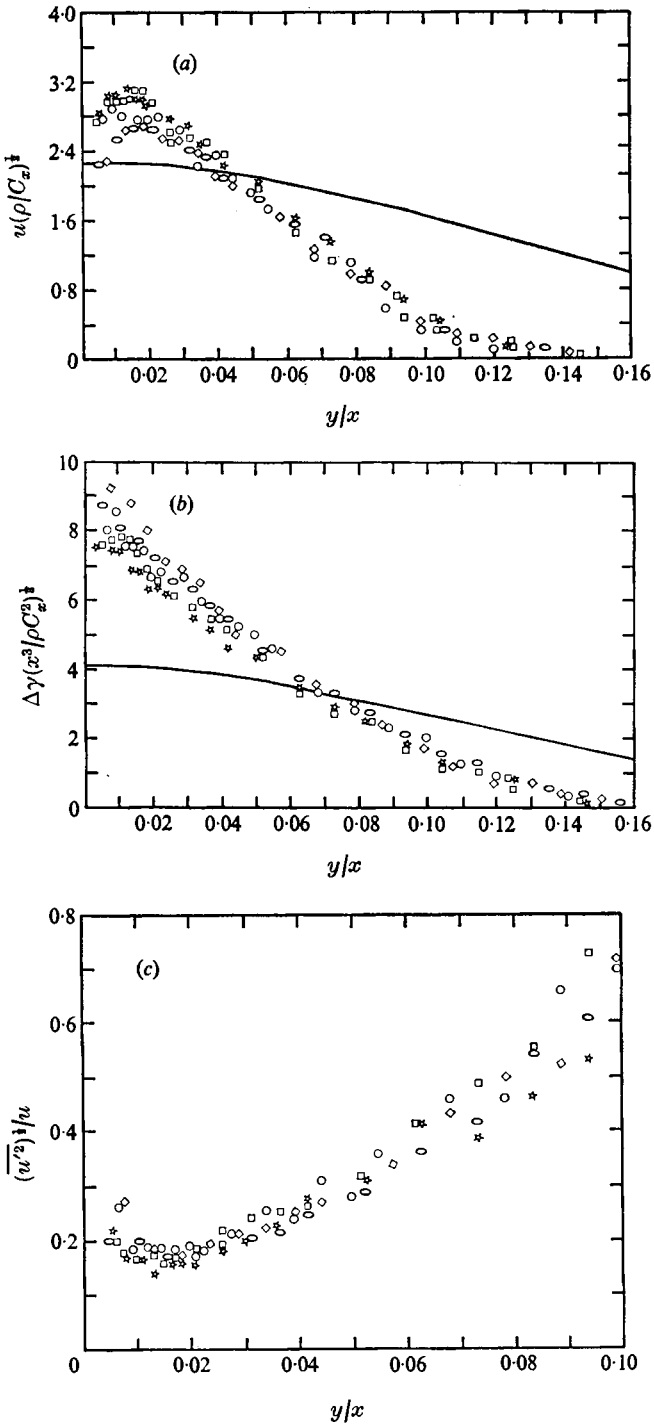

FIGURE 1. Distribution of (*a*) mean velocity, (*b*) weight density defect and (*c*) turbulent intensity in the adiabatic wall plume. Tests: ◇, 1; ○, 2; ○, 3; □, 4; ✲, 5. ——, unconfined line plume.

While the wall was essentially adiabatic for the conditions corresponding to figure 1 (*b*), the approach of the weight density defect profile to zero slope at the wall is not apparent. Seban & Back (1961) have observed similar behaviour for a two-dimensional adiabatic wall jet. They indicated that an approach to zero slope occurs very close to the wall owing to reduced turbulent transport in this region.

The vertical component of the local turbulence intensity could be determined with the single wire probe. These measurements are shown in figure 1 (*c*). This parameter shows greater similarity than mean quantities for these test conditions. The present intensity values are about half as large as those measured by Poreh *et al.* (1967) for a radial wall jet. The general shape of the present plot, however, is similar to that for the wall jet.

5. Integral and entrainment constants

The entrainment constant and the integrals of (11) were determined by integrating the profiles and averaging over the five sets of test conditions. Since the present velocity data were limited near the wall, a one-seventh power velocity variation was assumed between the wall and the maximum-velocity point in order to complete the integrations. In addition, the points where the velocity and weight density defect are half their maximum values, $\eta(\frac{1}{2}u_m)$ and $\eta(\frac{1}{2}\Delta\gamma_m)$, were also determined (with η taken as y/x). The average values of all these parameters and their standard deviations are given in table 2. The present measurements are also compared in table 2 with the earlier wall-plume results of Ellison & Turner (1959) and the results for unconfined line plumes of Rouse *et al.* (1952) and Lee & Emmons (1961). The line-plume results agree with each other very closely.

Since the definition of the length scale σ is arbitrary, I_1 may be set equal to E_0 without loss of generality. The entrainment constant of Ellison & Turner (1959) is based upon the average velocity of the flow and is related to E_0 as follows:

$$E_0' = E_0 I_1/I_2. \tag{14}$$

The values of this parameter for all four studies can be compared and are also listed in table 2.

The wall-plume values of E_0' are in fair agreement with each other, but are less than half the values for unconfined line plumes. Turner (1973) has suggested that the larger apparent entrainment of free plumes is due to large-scale wavering, or the regular swaying motion of these plumes. This type of behaviour has been observed by Forstrom & Sparrow (1967) for laminar line plumes. Differences in entrainment between wall and unconfined plumes are also to be expected owing to the wall boundary condition as opposed to that of a plane of symmetry.

The free-plume data can be represented by Gaussian velocity and weight density defect profiles. A Gaussian velocity profile gives a ratio of $2^{-\frac{1}{2}}$ for I_2/I_1, which is very close to the present wall-plume value even though the velocity profile is not Gaussian near the wall.

For Gaussian profiles, the ratio I_3/I_1 is equal to the ratio of the length scales

	Wall plumes		Unconfined line plumes	
	Present study	Ellison & Turner	Rouse *et al.*	Lee & Emmons
E_0, I_1	$0{\cdot}067 \pm 0{\cdot}004$	—	0·157	0·16
E_0'	$0{\cdot}095 \pm 0{\cdot}005$	$0{\cdot}087 \pm 0{\cdot}005$	0·222	0·226
I_2/I_1	$0{\cdot}701 \pm 0{\cdot}007$	—	0·707	0·707
I_3/I_1	$0{\cdot}937 \pm 0{\cdot}066$	—	0·883	0·900
I_4/I_1	$0{\cdot}617 \pm 0{\cdot}040$	—	0·661	0·669
$\eta(\frac{1}{2}u_m)$	$0{\cdot}066 \pm 0{\cdot}006$	—	0·147	—
$\eta(\frac{1}{2}\Delta\gamma_m)$	$0{\cdot}055 \pm 0{\cdot}002$	—	0·130	—

TABLE 2. Values of entrainment and integral constants for wall plumes and unconfined free plumes. Values from Ellison & Turner estimated from a plot

C_f	$u_m/(C_x\rho)^{\frac{1}{2}}$	$\Delta\gamma_m x/(C_x^2\rho)^{\frac{1}{2}}$	F_m
0	$3{\cdot}19 \pm 0{\cdot}08$	$7{\cdot}64 \pm 0{\cdot}27$	$5{\cdot}71 \pm 0{\cdot}24$
0·01	$3{\cdot}09 \pm 0{\cdot}07$	$7{\cdot}91 \pm 0{\cdot}25$	$5{\cdot}42 \pm 0{\cdot}20$

TABLE 3. Computed variation of dimensionless flow parameters with skin-friction coefficient

of the density defect and velocity profiles. The free-plume values of this ratio are approximately 0·9, indicating a more rapid spread of the velocity profile. This ratio is also less than unity for the wall plume. The greater width of the velocity profile is also indicated by the values of $\eta(\frac{1}{2}u_m)$ and $\eta(\frac{1}{2}\Delta\gamma_m)$ for the two flows.

6. Influence of wall friction

With the entrainment constant and the various integrals of the flow determined, the direct effect of wall friction can be estimated through (12) and (13). Two cases, involving values of 0 and 0·1 for C_f, are considered. The latter value is chosen to be representative of a smooth wall with a high ambient turbulent intensity in the Reynolds number range of the present experiments. The former value is representative of asymptotic behaviour at large Reynolds numbers. The results are given in table 3, along with the standard deviation of each value for the five tests.

The effect of friction-factor variation is not very large over the range considered in table 3. The frictional case provides a 3 % reduction in the maximum velocity with a comparable increase in the maximum weight density defect. The presence of wall friction reduces the local Froude number by about 5 %.

The values of the dimensionless maximum velocity and weight density defect given in table 3 are in good agreement with the data for the higher test position in figures 1 (*a*) and (*b*). Also, the computed local Froude numbers in table 3 agree with the directly observed values for the data for the higher test position in table 1. This indicates a reasonable degree of internal consistency for these

results. The results at the lower position are in poorer agreement. This could be due to flow-development effects, a wall layer that was not fully turbulent or the lower experimental accuracy in the narrower plume at this position.

7. Conclusions

Mean velocities and weight density defects were measured within an adiabatic plume on a vertical wall. In agreement with earlier results, the rate of entrainment of the wall plume is substantially below that of unconfined line plumes. This results in higher velocities and greater weight density defects (or temperature rises in a thermal plume) in the wall plume than in a free plume under comparable conditions. In both the wall and unconfined line plume, however, the characteristic width of the velocity profile is larger than that of the weight density defect profile. The shape of the turbulent intensity profile is similar to that of a wall jet, but the intensity values are about half as large.

The magnitude of the wall friction factor does not have a large influence on conditions within the plume. A decreasing friction factor causes a slight increase in the velocity and a slight reduction in the density defect under the assumption of fixed values for the entrainment and integral constants. The observed variation of these parameters was greater than that anticipated from the estimated friction-factor variation; however flow-development effects and reduced experimental accuracy could have contributed to this apparent behaviour.

REFERENCES

Cheesewright, H. 1968 *J. Heat Transfer*, **90**, 1.

Ellison, T. H. & Turner, J. S. 1959 *J. Fluid Mech.* **6**, 423.

Forstrom, R. J. & Sparrow, E. M. 1967 *J. Heat Mass Transfer*, **10**, 321.

Fox, D. G. 1970 *J. Geophys. Res.* **75**, 6818.

Lee, S. L. & Emmons, H. W. 1961 *J. Fluid Mech.* **11**, 353.

Lockwood, F. C. & Ong, P. H. 1972 In *Heat and Mass Transfer in Boundary Layers*, vol. 1 (ed. N. Afgan, Z. Zaric & P. Anastasijevic), p. 340. Pergamon.

Morton, B. R. 1959 *J. Fluid Mech.* **5**, 151.

Morton, B. R., Taylor, G. I. & Turner, J. S. 1956 *Proc. Roy. Soc.* A **234**, 1.

Narain, J. P. & Uberoi, M. S. 1974 *J. Appl. Mech.* **41**, 337.

Poreh, M., Tsuei, Y. G. & Cermak, J. E. 1967 *J. Appl. Mech.* **89**, 457.

Rouse, H., Yih, Y. S. & Humphreys, H. W. 1952 *Tellus*, **4**, 201.

Seban, R. A. & Back, L. H. 1961 *Int. J. Heat Mass Transfer*, **3**, 255.

Turner, J. S. 1973 *Buoyancy Effects in Fluids*, p. 165. Cambridge University Press.